catalysts

MDPI

Supplementary Materials

Removal of some pharmaceuticals by photolysis and photocatalysis from water: Kinetic models

Miguel A. Jiménez-López, María C. Rubio-Gonzaga and Fernando J. Beltrán *.

Departamento de Ingeniería Química y Química Física, Instituto Universitario de Investigación del Agua, Cambio Climático y Sostenibilidad (IACYS), Universidad de Extremadura, Avenida de Elvas s/n, 06006 Badajoz, Spain; majimlopez@unex.es (M.A.J.-L); mrubiowz@alumnos.unex.es (M.C.R.-G); fjbeltran@unex.es (F.J.B.)

* Correspondence: fjbeltran@unex.es; Tel.: 34-924-289387

1. Experimental conditions and results reported in studies related to the topic.

Table S1. Key results and experimental conditions from references related to the TiO_2-photocatalytic removal of the selected compounds.

Comp.	Photocatalyst	Radiation Type	Initial Conc. ($mg \cdot L^{-1}$)	Cat. Dose ($g \cdot L^{-1}$)	Irradiation Time (min)	Removal (%)	TOC Reduction (%)	Ref.
ATL	No photocatalyst	UVC (254 nm) (15W)	5	--	60	62	<13	[1]
	TiO_2/NCP	UV (60 W)	10.0	3.0	60.0	75.0	74	[2]
	TiO_2/SN-MIL-101(Cr)	Visible (Xe lamp, 100 W)	10.0	1.5	60.0	82.0	82	[2]
	TiO_2 P25 (pilot-scale)	Natural sunlight (solar CPCs)	10.0	0.2	33.4	100.0	40	[3]
ACM	No photocatalyst	UVC (254 nm) (15W)	5	--	60	54	<13	[1]
	$TiO_2/KAl(SO_4)_2$	LED (440–490 nm) (5W)	15.1	1.0	540.0	95.0	n.r.	[4]
	Degussa P-25		15.1	1.0	540.0	65.0	n.r.	[4]
	$TiO_2/NaAlO_2$		15.1	1.0	540.0	50.0	n.r.	[4]
	Undoped TiO_2		15.1	1.0	540.0	32.0	n.r.	[4]
	Montmorillonite-TiO_2 nanosheets	UV (254 nm) (282–294 W/m^2)	2.0	0.75	120.0	100.0	n.r.	[5]
CLA	No photocatalyst	UVC (254 nm) (40 W)	2.14	--	60	91.9	n.r.	[6]
	Pd-doped TiO_2	UV-A (365 nm) (6.2 mW/cm^2)	5	0.2	50.0	100	65	[7]
			25	0.2	110.0	100	32	[7]
	TiO_2 (sol–gel, calcined at 673 K)	Visible (366 nm, filtered mercury lamp) (150 W)	18	1.0	240.0	100	79.4	[8]
ANT	No photocatalyst	UVC (254 nm) (15W)	5	--	60	40	n.r.	[9]
	UV/H_2O_2 0.5 mM H_2O_2					>95	n.r.	
	UV/PS 0.5 mM persulfate					>95	n.r.	
	TiO_2-AZA4 (azaindole-grafted TiO_2)	Simulated solar irradiation ($\lambda \geq 320$ nm, 600 W/m^2)	5	0.25	1200.0	55	n.r.	[10]

n.r.: not reported.

2. Absorption spectra for pharmaceuticals and scavengers

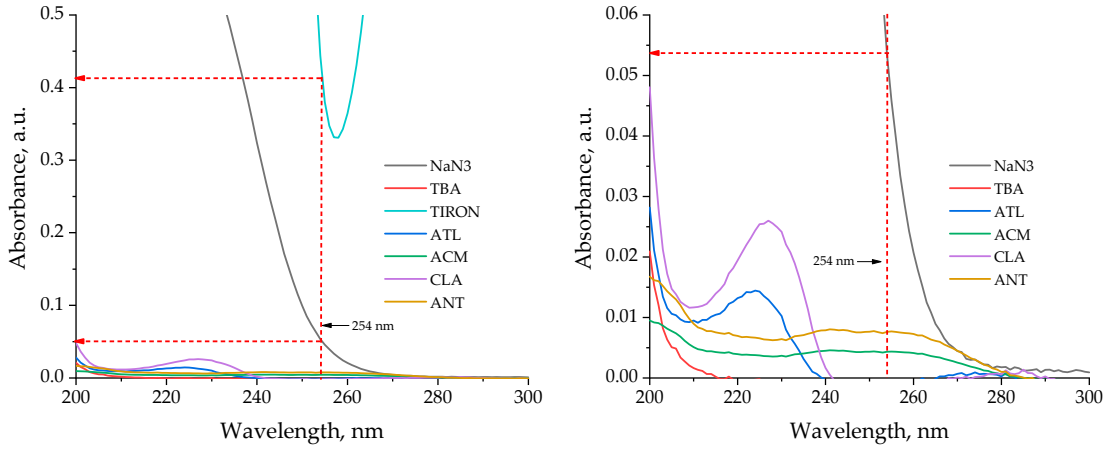

Figure S1. Comparison of initial scavenger and pharmaceutical absorbance at 254 nm. Conditions: C_{Pharm} = 0.5 ppm, C_{Tiron0}=0.001 M, $C_{TBA,0}$ = 0.01 M, $C_{NAN3,0}$ = 0.01 M.

3. Wastewater effluent quantum yield at 254 nm and its time evolution absorbance at this wavelength

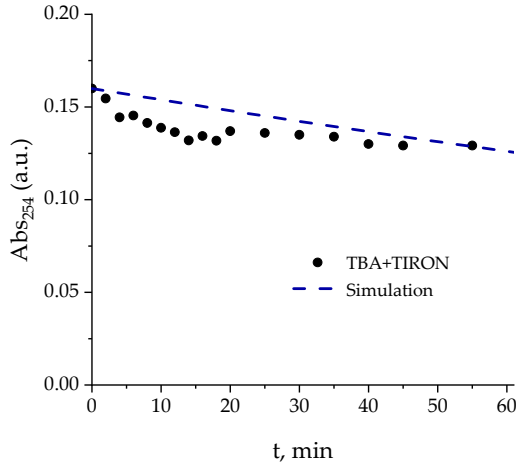

Figure S2. Fit of absorbance at 254 nm of wastewater effluent with time using the analytical solution of Equation (5), employing the quantum yield value calculated from experiments with TBA and TIRON. Initial conditions: Abs_{2540} = 0.160 a.u., C_{Tiron0}=0.001 M, $C_{TBA,0}$ = 0.01 M pH_0 = 7.

4. Determination of apparent and direct quantum yields of pharmaceuticals at 254 nm

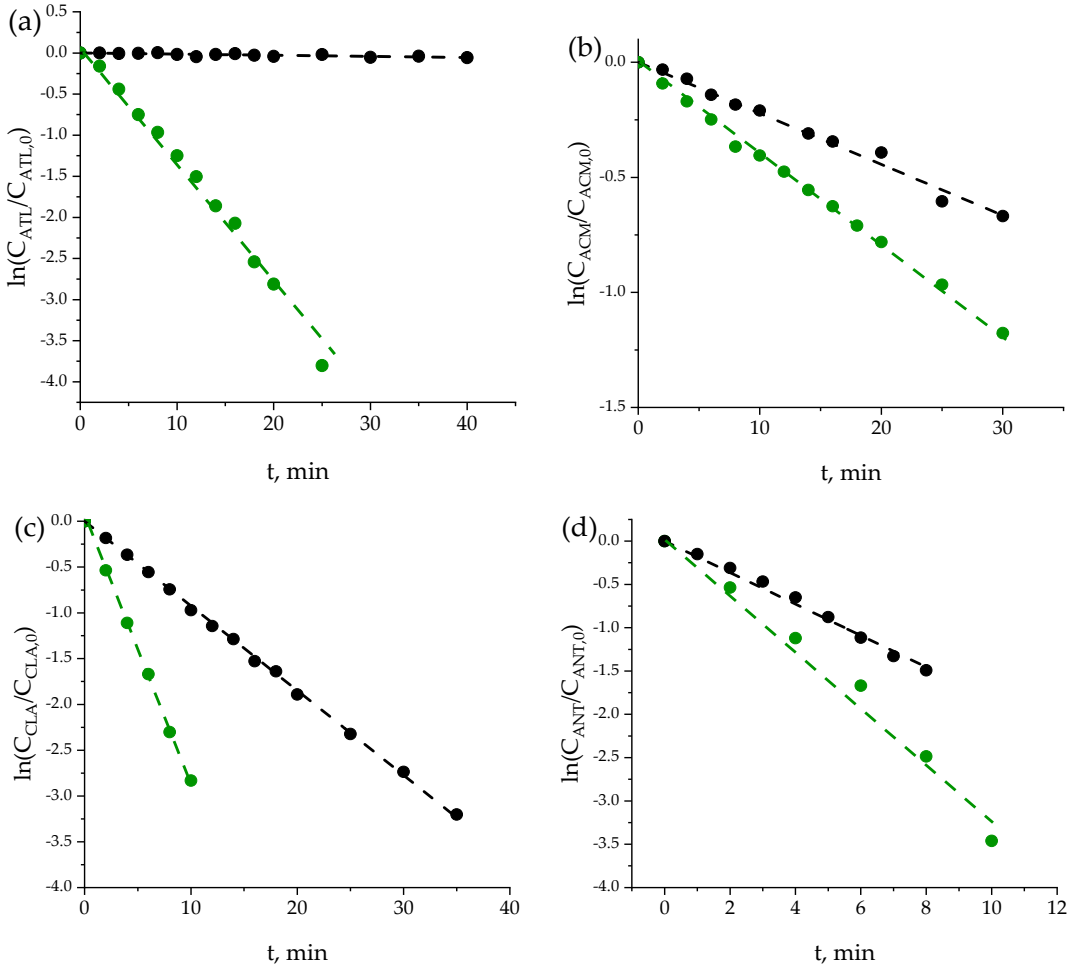

Figure S3. Fitting equation (3) to the experimental photolysis data: (a) ATL, (b) ACM, (c) CLA, (d) ANT. Conditions as in Figure 2. Green line: without scavengers; black line: with TBA and TIRON.

5. Determination of rate constant of singlet oxygen-pharmaceutical reactions

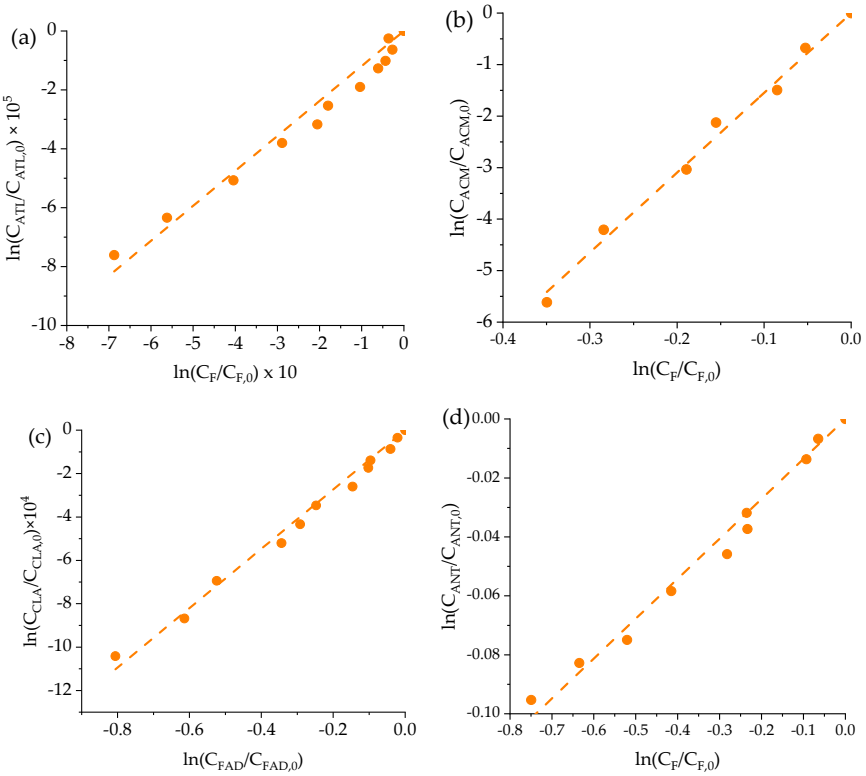

Figure S4. Evaluation of Equation (4) based on the experiments with Rose Bengal. ATL, (**b**) ACM, (**c**) CLA, (**d**) ANT. Determination of the singlet oxygen-pharmaceutical reaction rate constant.

6.-Kinetic parameters and rate constants used in the photolysis model[a]

Table S2. Kinetic parameters and rate constants used in the photolysis model[a].

Pharmaceuticals	k_{HOM}	$k_{O2^{\bullet-}}$	k_H	k_F	k_T[b]	α[c]	β[d]
	$M^{-1}\cdot s^{-1}$	$M^{-1}\cdot s^{-1}$	$M^{-1}\cdot s^{-1}$	$M^{-1}\cdot s^{-1}$	s^{-1}		
ATL	2.2×10^9	4.0×10^6	2.71×10^7	5.0×10^9	5×10^3	1.8	0.05
ACM	1.6×10^9	4.0×10^6					
CLA	2.7×10^9	1.0×10^8					
ANT	9.0×10^8	2.0×10^6					

[a]Io=3.99×10^{-6} EinsteinL^{-1}s^{-1}. ϕ_{WWEf} = 5.53 a.u.L^{-1}Einstein^{-1}. For other parameters and rate constants, see Tables 1 to 3. [b]For the case of WWEf. [c]$mol_{HO\bullet}(mol_{ATL+ACM})^{-1}$. [d]$mol_{1O2}(mol_{CLA+ANT})^{-1}$.

7. Comparison of mineralisation rates depending on the concentration of photocatalyst applied

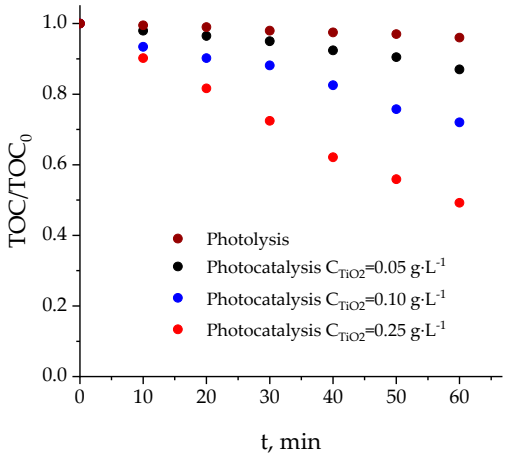

Figure S5. Total organic carbon (TOC) removal during photolysis and photocatalysis of the mixture of pharmaceuticals in effluent wastewater: experimental results. Conditions: C_{Pharm0} = 0.5 mg·L^{-1}, pH_0 = 7, Io = 3.99 × 10^{-6} Einstein·L^{-1}s^{-1}, TOC_0 = 8.52 mg·L^{-1}.

8. Comparison of experimental and calculated concentrations of pharmaceuticals without considering the effect of end free radical reactions

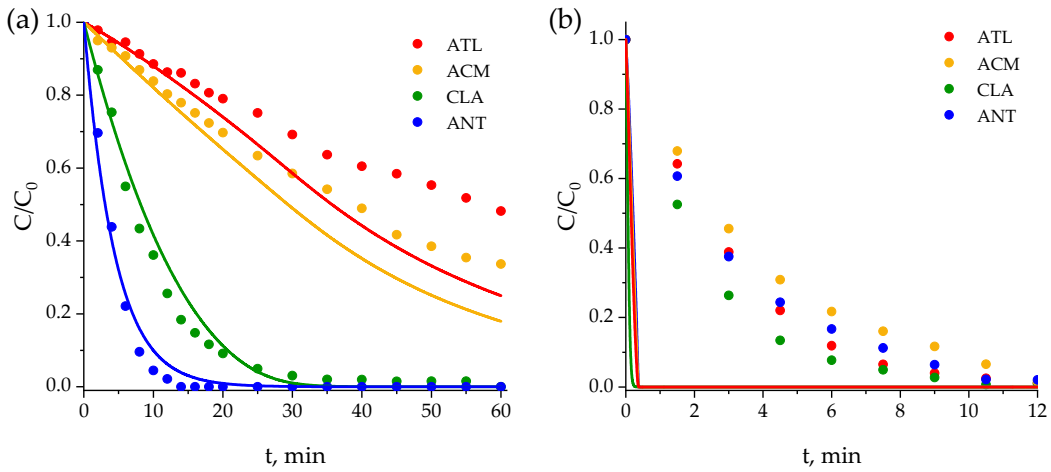

Figure S6. Experimental degradation profiles (symbols) in secondary effluent under (a) photolytic (UVC) and (b) photocatalytic (UVC/TiO_2) conditions. Solid lines represent simulation results obtained without including termination and intermediate degradation reactions in the kinetic model.

9. Kinetic parameters and rate constants used in the photocatalysis model

Table S3. Kinetic parameters and rate constants used in the photocatalysis model[a]

C_{TiO2} g·L^{-1}	$k_{HOs\text{-}M} \times 10^{-9}$ ($M^{-1}\cdot s^{-1}$)				$k_T \times 10^{-5}$ (s^{-1})	$k_{TT} \times 10^{-2}$ (s^{-1})	$r_0 \times 10^{6}$ (Einstein$L^{-1}s^{-1}$)
	ATL	ACM	CLA	ANT			
0.05	1.1	0.8	0.1	0.5	1.3	10	1.52
0.10	2.2	1.6	0.1	1.8	1.8	8	3.04
0.25	5.5	4.0	0.1	4.5	3.0	3	3.99

[a]From [11]: k_{1s}=5 × 10^{11} s^{-1}, k_{rec}=6.3 × 10^{30} $M^{-1}{}_{eq}s^{-1}$, k_e=1.9 × 10^{10} $M^{-1}{}_{eq}s^{-1}$, k_{eH}=1.1 × 10^{10} in $M^{-1}{}_{eq}\cdot s^{-1}$

10. Characterization of wastewater effluent

Table S4. Chemical characterization of secondary effluent

Parameter	Value
pH	7.2
Turbidity (NTU)	3.72
Conductivity (μS·cm^{-1})	498
A254 (a.u.)	0.16
SUVA (L·$mg^{-1}\cdot m^{-1}$)	2.19
IC (mg·L^{-1})	27.6
TOC (mg·L^{-1})	7.3
F^- (mg·L^{-1})	0.1
Cl^- (mg·L^{-1})	53
NO_2^- (mg·L^{-1})	0.4
NO_3^- (mg·L^{-1})	4.2
PO_4^{3-} (mg·L^{-1})	0.7
SO_4^{2-} (mg·L^{-1})	34

References

1. Katsumata, C.P.; Parizi, M.P.S.; Lastre-Acosta, A.M.; Teixeira, A.C.S.C. Low Pressure UV Photolysis of the Pharmaceutical Compounds Acetaminophen, Atenolol, Bezafibrate, Diclofenac and Ibuprofen. *Water (Switzerland)* **2022**, *14*, 3165, doi:10.3390/w14193165.
2. Mehrabadi, Z.; Faghihian, H. Comparative Photocatalytic Performance of TiO2 Supported on Clinoptilolite and TiO2/Salicylaldehyde-NH2-MIL-101(Cr) for Degradation of Pharmaceutical Pollutant Atenolol under UV and Visible Irradiations. *J Photochem Photobiol A Chem* **2018**, *356*, 102–111, doi:10.1016/J.JPHOTOCHEM.2017.12.042.
3. Radjenović, J.; Sirtori, C.; Petrović, M.; Barceló, D.; Malato, S. Solar Photocatalytic Degradation of Persistent Pharmaceuticals at Pilot-Scale: Kinetics and Characterization of Major Intermediate Products. *Appl Catal B* **2009**, *89*, 255–264, doi:10.1016/j.apcatb.2009.02.013.
4. Dalida, M.L.P.; Amer, K.M.S.; Su, C.C.; Lu, M.C. Photocatalytic Degradation of Acetaminophen in Modified TiO2 under Visible Irradiation. *Environmental Science and Pollution Research* **2014**, *21*, 1208–1216, doi:10.1007/S11356-013-2003-4/FIGURES/10.
5. Shahabi, H.; Allahrasani, A.; Naghizadeh, A. Photocatalytic Degradation of Acetaminophen in Aqueous Solution in the Presence of Montmorillonite Nanosheets Modified with Titanium Dioxide. *Desalination Water Treat* **2019**, *149*, 164–170, doi:10.5004/DWT.2019.23794.
6. Li, W.; Lu, S.; Qiu, Z.; Lin, K. Clofibric Acid Degradation in UV254/H2O2 Process: Effect of Temperature. *J Hazard Mater* **2010**, *176*, 1051–1057, doi:10.1016/j.jhazmat.2009.11.147.
7. Harja, M.; Sescu, A.M.; Favier, L.; Lutic, D. Doping Titanium Dioxide with Palladiun for Enhancing the Photocatalytic Decontamination and Mineralization of a Refractory Water Pollutant. *Revista de Chimie* **2020**, *71*, 145–152, doi:10.37358/RC.20.7.8232.
8. Silva, C.G.; Faria, J.L. Anatase vs. Rutile Efficiency on the Photocatalytic Degradation of Clofibric Acid under near UV to Visible Irradiation. *Photochemical and Photobiological Sciences* **2009**, *8*, 705–711, doi:10.1039/B817364H/METRICS.
9. Tan, C.; Gao, N.; Deng, Y.; Zhang, Y.; Sui, M.; Deng, J.; Zhou, S. Degradation of Antipyrine by UV, UV/H2O2 and UV/PS. *J Hazard Mater* **2013**, *260*, 1008–1016, doi:10.1016/j.jhazmat.2013.06.060.
10. Peñas-Garzón, M.; Gómez-Avilés, A.; Álvarez-Conde, J.; Bedia, J.; García-Frutos, E.M.; Belver, C. Azaindole Grafted Titanium Dioxide for the Photodegradation of Pharmaceuticals under Solar Irradiation. *J Colloid Interface Sci* **2023**, *629*, 593–603, doi:10.1016/j.jcis.2022.09.005.
11. Beltrán, F.J.; Jiménez-López, M.A.; Álvarez, P.M.; Rivas, F.J. Kinetic Modeling of Photocatalytic Oxidation-Ozonation of Metronidazole Removal from Water. *J Environ Chem Eng* **2025**, *13*, 115869, doi:10.1016/J.JECE.2025.115869.